High-cycle-fatigue induced continuous grain growth in ultrafine-grained titanium

P. Zhao[a], B. Chen[b,c*], J. Kelleher[d], G. Yuan[a], B. Guan[e], X. Zhang[a,**], S. Tu[a]

[a]*Key Laboratory of Pressure Systems and Safety, Ministry of Education, School of Mechanical and Power Engineering, East China University of Science and Technology, Shanghai 200237, China*

[b]*Department of Engineering, University of Leicester, Leicester, LE1 7RH, UK*

[c]*Faculty of Engineering, Environment and Computing, Coventry University, Coventry, CV1 5FB, UK*

[d]*ISIS, Science and Technology Facilities Council, Rutherford Appleton Laboratory, Chilton, Didcot OX11 0QX, UK*

[e]*National Engineering Research Center for Magnesium Alloys, Chongqing University, Chongqing, 400044, China*

*Corresponding authors. E-mail address: *bo.chen@leicester.ac.uk, **xczhang@ecust.edu.cn

Abstract

The cyclic deformation behaviour and microstructural stability of severe plastic deformation processed bulk nanostructured (ultrafine-grained, UFG) commercially pure cp-Ti were investigated by using *in situ* neutron diffraction combined with R=-1 high-cycle-fatigue (HCF) loading at room and cryogenic temperatures. The UFG microstructure was created by equal channel angular pressing (ECAP) and multi-direction forging (MDF). A considerable continuous grain growth was revealed by neutron diffraction for MDF cp-Ti fatigued at 25 °C, as opposed to that at -200 °C. The same HCF fatigue loading at 25 °C only caused very limited grain growth for ECAP cp-Ti. Transmission electron microscopy confirmed the grain growth. Further confirmation of the room-temperature HCF fatigue-induced grain growth was obtained by transmission Kikuchi diffraction based analysis. Novel insights into fatigue induced grain growth mechanism in UFG cp-Ti are thus provided: (i) the thermally activated process plays an important role in grain growth during the room-temperature HCF fatigue; (ii) Continuous dynamic recrystallisation is responsible for the grain growth and dislocation slip or twinning is not essential to trigger such a grain growth; (iii) the anisotropic grain growth behaviour in {0002} grain family can be reconciled by accepting that these grains accumulated highly

stored energy during initial severe plastic deformation and the subsequent recrystallisation nucleation occurred at these highly deformed regions.

Keywords: Grain Growth, Fatigue, Texture, Titanium, Nanostructured metals, Neutron diffraction

1. Introduction

Grain refinement by severe plastic deformation (SPD) is widely used to process bulk nanostructured ultrafine-grained (UFG) metals [1]. Similar to improved static strength, the high-cycle-fatigue (HCF) of UFG [2] and nanocrystalline (NC) [3] metals has been recognised to be enhanced compared to coarse-grained counterparts. The enhanced fatigue limit can be attributed to a shift of the onset of micro-plasticity to higher stress levels [4]. However, the fatigue behaviour of UFG metals depends not only on the grain-size related strength but also on other characteristics of cyclic deformation and damage processes such as deformation induced grain coarsening [5–7] and fatigue crack promoted grain growth [3,8,9]. It has been suggested that a certain fatigue time and cumulative strain are required for the release of stored strain energy to trigger dislocation motion, recrystallisation and associated grain growth [7], as well as crack initiation [5].

Witney et al. [6] performed the first fatigue study on NC copper that was processed by inert gas condensation. A grain growth of 30% in size was found after 10^5 cycles under tension-tension cyclic loading (stress ratio of R=0.1). Inert gas condensation has known limitations that include small sample dimensions and remained porosities [10]. These drawbacks mean that performing fatigue tests using standard bulk specimens particularly with tension-compression HCF (e.g. R=-1) would be almost impossible. Equal channel angular pressing (ECAP) is one of the SPD methods to fabricate bulk nanostructured samples by imposing severe plastic straining. Another method is multi-directional forging (MDF). Both ECAP and MDF can produce bulk sample with the fully dense UFG microstructure [1]; in the present work they were used to fabricate commercially pure titanium cp-Ti.

For prospective engineering applications of UFG metals processed by SPD, the fatigue behaviour and microstructural stability must be understood thoroughly. Vinogradov and Hashimoto [11] commented that the HCF life was enhanced for nanostructured ECAP titanium when compared to fine-grained counterpart. However, later fatigue data on ECAP copper seem contradictory. Hoppel et al. [7] performed both room-temperature and -50 °C stress-controlled HCF and strain-controlled low-cycle-fatigue (LCF) tests on ECAP copper. It was concluded that the grain growth was thermally activated because the grain coarsening was much less at -50 °C when

compared to room temperature. The grain growth in fatigued UFG copper was thus claimed to be a thermally activated recrystallisation process which occurred already at room temperature and was enhanced by lower cyclic strain rates [7].

Grain growth is often associated with thermally activated grain boundary migration, but it was also observed in NC copper strained at liquid-nitrogen temperature [12]. In detail, a faster grain growth under indentation loading at cryogenic temperature was found when compared to that at room temperature, suggesting that the grain growth is primarily stress-driven, not diffusion-driven. However, the detailed mechanism of grain growth in the complex and large stress/strain field of the indenter is not yet known. Boyce and Padilla [3] studied room-temperature fatigue-induced grain growth in NC nickel in which abnormal grain growth, close to crack initiation region, was claimed to be an evidence to support non-diffusional stress-driven process. They further postulated that such fatigue-induced grain growth was fundamentally distinct from dynamic recrystallisation. However, the nature of the grain growth process in UFG and NC metals is not completely agreed, especially considering some experimental evidence to support that diffusional process should play a certain role on grain growth in nanostructured metals. When a dynamic compression load was applied to ECAP titanium at -180 °C, transmission electron microscopy (TEM) confirmed the absence of grain growth [13]. In another work, residual indents resulting from room-temperature nano-indentation were studied by TEM to confirm the microstructural stability of NC platinum films [9].

Therefore, it remains an open question what is the individual role of thermal and mechanical stress-driven grain growth in nanostructured metals in response to HCF fatigue loading. Whether grain growth is continuous or discontinuous, whether a certain incubation time is required, and whether grains with certain crystallographic orientations grow preferentially, are still unclear. With the aforementioned background, the focus of the present work is twofold: (i) fully characterising the grain growth during a R=-1 HCF fatigue loading of UFG cp-Ti and (ii) decoupling the mechanical stress and temperature-dependent contributions to the overall grain growth by comparing room-temperature (25 °C) HCF with that performed at cryogenic temperature (liquid helium, -200±2 °C). Note that the applied stress amplitude was less than 50% of the macro-scopic yield strength of UFG cp-Ti to minimise the effects of dislocation slip and deformation twinning. *In situ* neutron diffraction measurements combined with HCF fatigue loading were performed to reveal the

cycle-dependent grain growth process. Post-mortem microstructural characterisations were carried out to validate and interpret the experimental observation.

2. Material and Experimental

2.1 Equal channel angular pressing (ECAP) and multi-directional forging (MDF)

The experiments used cp-Ti (ASTM grade 2) that has a single α-phase hexagonal close-packed (hcp) crystal structure in as-received condition. The chemical composition (wt. %) of the cp-Ti is Fe 0.28%; C 0.08%; N 0.03%; H 0.015%, O 0.25% and Ti in balance. Metallographic samples were polished down to OPS with colloidal silica, followed by etching with Kroll's reagent (2% HF, 6% HNO_3 and 92% H_2O). The grain size was measured to be 35±15 μm by using linear intercept method.

The UFG cp-Ti samples were processed by using ECAP and MDF methods. Compared to MDF, ECAP can process a relatively large volume of titanium billet (50×50×100 mm), hence enabling several bulk mechanical testing specimens extracted from one ECAP-deformed sample block. Pressing was applied with a constant displacement rate of 10 mm/s following route C (i.e. after each pass the billet was rotated 180° around its longitudinal axis.) [1]. Both the cp-Ti billet and die were heated to 450 °C and isothermally held within ±2 °C for at least 40 mins prior to ECAP. The solid die had an angle of 90° between the two adjacent channels. To ensure the process temperature of 450 °C, the cp-Ti billet was re-heated after four passes. The temperature selection was according to previous work [14]. The cp-Ti billet was processed through totally twelve passes. The final dimensions of ECAP cp-Ti was approx. 50×50×80 mm and the sample surface was crack-free. The magnitude of equivalent strain for the ECAP cp-Ti was estimated as ~14 according to [15].

In terms of MDF, the as-received cp-Ti with dimensions of 35 mm in diameter and 60 mm in length was used. The sample was pre-heated to 450 °C, followed by high-strain rate forging from three orthogonal directions. The stroke speed of the pneumatic hammer (65 kg in weight) used to deform the sample was approx. 5 to 6 hitting times per second, resulting in a very high-strain rate of 20 s^{-1}. For each cycle, the hammer force was applied along three individual orthogonal directions to deform the material. In total three MDF cycles were used to introduce an equivalent strain of

~5. The final dimensions of MDF-deformed cp-Ti sample were 23×25×90 mm. The primary difference between ECAP and MDF lies with the deformation rate; the strain rate for the latter was two orders of magnitude higher than the former.

2.2 *In situ* neutron diffraction measurement combined with HCF fatigue loading

To gain a better understanding about the grain growth behaviour of UFG cp-Ti under HCF fatigue loading, a suitable experimental technique is required. While TEM can supply detailed information about grain size over a relatively small sample area, neutron diffraction used in the present work can supply *in situ* information about the volume-average grain size change and texture evolution, hence providing statistically significant data. To this end, both MDF and ECAP cp-Ti were subjected to HCF fatigue under fully reversed tension-compression (R=-1) loading where neutron diffraction measurements were performed at interrupted fatigue cycles of 0 (reference condition), 10^1, 10^2, 10^3, 10^4, 10^5, 2×10^5; all at the unloaded state.

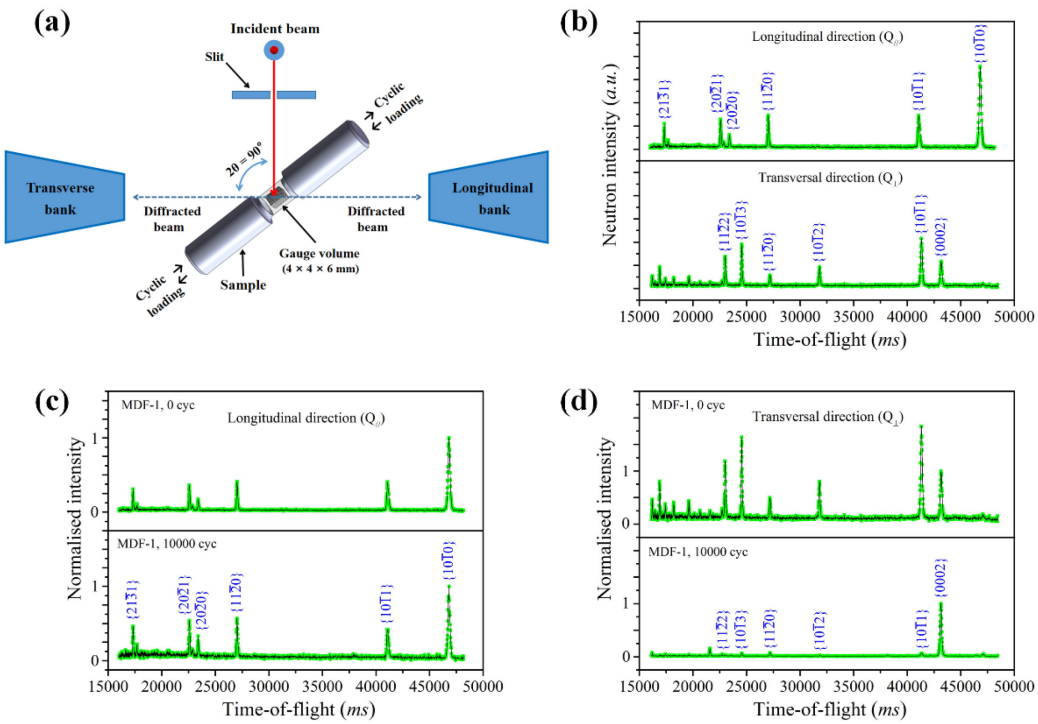

Figure 1: (a) Arrangement of the fatigue specimen in ENGIN-X for measurements along both longitudinal and transversal directions; (b) a comparison of two diffraction spectra obtained from both directions for the pre-fatigued MDF-1 showing the initial texture; (c) and (d) comparisons of pre- and post-fatigued MDF-1 for longitudinal and transversal directions respectively. Note: Diffraction spectra in (c) and (d) were normalised against $\{10\bar{1}0\}$ for longitudinal and $\{0002\}$ for transversal direction.

A time-of-flight neutron diffractometer, ENGIN-X, at ISIS in the UK, combined with a horizontal Instron servo-hydraulic fatigue loading rig as well as a cryogenic box, was used for the *in situ* work. Two detector banks, located at Bragg angles $2\theta=\pm 90°$ relative to the incident neutron beam respectively, provided a measure of full time-of-flight diffraction spectrum along both the longitudinal and transversal directions simultaneously as shown in Fig. 1a. The HCF fatigue tests were conducted at both 25 °C and -200±2 °C in a helium cryogenic environment.

Cylindrical samples were extracted from the ECAP and MDF-deformed cp-Ti billets with a gauge length of 14 mm and diameter of 8 mm, and with the fatigue loading axis parallel to the longitudinal direction of the billet. Sample surfaces within the gauge were polished to a surface roughness of 0.3 μm. The gauge volume selected for the neutron diffraction measurement was 4×4×6 mm (where 6 mm is along the longitudinal direction) at the centre position of the sample, see Fig. 1a. The data collection time was 25 mins per measurement to achieve a good statistical quality of the diffraction peak fit.

The constant stress amplitude of 280 MPa was applied with triangular waveforms for HCF fatigue tests using a frequency of 14 Hz. The magnitude of fatigue stress amplitude was determined based on tensile yield strength that had been derived based on the tensile strain rate of 3×10^{-4} s^{-1} at room temperature. The applied fatigue stress was lower than 50% of the macro-scopic yield strength for both MDF and ECAP cp-Ti, Table 1. In total, three *in situ* fatigue samples were studied, Table 2. Specimens MDF-1 and MDF-2 were tested at 25 °C and -200 °C respectively, while ECAP was tested at 25 °C. In order to verify the repeatability of the *in situ* work, two off-line room-temperature fatigue tests on MDF cp-Ti were performed. These two specimens were stopped at cycles of 10^2 and 10^3, followed by examining the grain size and micro-hardness.

Table 1. Tensile properties of as-received and severe plastic deformed cp-Ti samples

Sample condition	Elastic limit (MPa)	Yield strength (MPa)	Tensile strength (MPa)	Elongation (%)
As-received	303	325	416	34
ECAP	544	597	654	25
MDF	570	613	705	22

Table 2. HCF fatigue samples combined with neutron diffraction (ND) measurements

Sample ID	Grain size	Temperature	Stress amplitude (R=-1)	Final registered fatigue cycles with ND
MDF-1	253 nm	25 °C	280 MPa	1×10^4
MDF-2		-200 °C		2×10^5
ECAP	638 nm	25 °C		1×10^4

Fig. 1b illustrates typical neutron diffraction spectra obtained from longitudinal and transversal directions for pre-fatigued MDF-1. Both the Pawley fitting (Rietveld refinement) and single-peak fitting routines, available at ENGIN-X, were used to process the diffraction data. In the Pawley fitting, the unit cell, zero point and peak profile parameters were varied in least-squares fit to the diffraction data [16] and more details can be found in [17]. From the expression for the Gaussian broadening of time-of-flight diffraction peaks (the complete diffraction spectrum), the peak width broadening as manifested by the profile coefficient σ_{gauss} is inversely proportional to the average crystallite size, i.e. a grain size increase would correspond to a decreased σ_{gauss} value. This is according to the classic Scherrer formula for X-ray particle size determination [18]. In terms of single-peak fitting, six grain families from hcp α-phase Ti were considered for longitudinal direction: $\{10\bar{1}0\}$, $\{10\bar{1}1\}$, $\{11\bar{2}0\}$, $\{20\bar{2}0\}$, $\{20\bar{2}1\}$ and $\{21\bar{3}1\}$, while $\{0002\}$, $\{10\bar{1}1\}$, $\{10\bar{1}2\}$, $\{11\bar{2}0\}$, $\{10\bar{1}3\}$ and $\{11\bar{2}2\}$ grain families for the transversal direction, Fig. 1b. A similar ENGIN-X *in situ* experimental set up and peak analysis can be found elsewhere [19,20].

2.3 Microstructural characterisation

The grain size distribution of ECAP and MDF cp-Ti before and after *in situ* HCF fatigue were examined by using JEM-2100 TEM operating at 200 kV. The TEM thin foils were mechanically ground and then twin jet thinned in an electrolytic solution of 4% perchloric acid + 96% alcohol at -30 °C with a voltage of 75 V and a current of 50 mA. The mean grain size, $\bar{D}$, was determined using both linear intercept method and individual average length determination by counting >300 grains under bright-field TEM micrographs. The grain coarsening study by Ferry and Burhan [21] on a UFG aluminium showed that lognormal distribution was the best fit to the measured grain sizes. A similar statistical approach to present size distribution of a

microstructural feature (α-lath width in Ti-6Al-4V alloy) was described in [22], Here, we adopted the same method to present the grain size-distribution histogram.

The change in the fraction of high-angle grain boundaries (HAGBs) relative to low-angle grain boundaries (LAGBs) is of particular importance in determining whether a continuous or discontinuous recrystallisation is responsible for the grain growth [23]. Electron backscattered diffraction (EBSD) was used to quantify them. The microstructure of the MDF-deformed cp-Ti was studied by using a Zeiss AURIGA FIB-SEM workstation equipped with transmission Kikuchi diffraction, TKD capability. The main advantage of TKD over the conventional EBSD* is to offer a significantly higher spatial resolution [24], which is thus more suitable for the UFG cp-Ti. The TEM thin foils prepared from the MDF-deformed cp-Ti in both pre- and post-fatigued conditions were used for TKD characterisation. All TKD scans were performed at 30 kV and a step size of 50 nm with the sample pre-tilt angle of -20°. The TKD maps were subsequently analysed by Channel 5 software. The microtexture was determined from TKD orientation maps to confirm the neutron diffraction measurement from both the longitudinal and transversal detector banks.

Micro-hardness measurements were performed on HXD-1000TM/LCD tester at a load of 0.98 N for 15 s per indent. A mean value out of 10 individual measurements is presented. The microstructural characterisations as well as micro-hardness were made on the cross-sectional plane (unless stated otherwise). Hence the microstructural information obtained is directly related to the neutron diffraction data collected along the longitudinal direction, namely the longitudinal bank of Fig. 1a.

3. Results

3.1 Grain refinement by ECAP and MDF

Representative TEM micrographs are shown in Fig. 2a and 2c for MDF and ECAP cp-Ti respectively. The microstructure consists of near-equiaxed UFG grains with a mean grain size $\overline{D}$ of 253 nm for MDF and 638 nm for ECAP cp-Ti. The inset in Fig. 2a provides a clearer illustration of a much finer UFG microstructure created by MDF. The presence of a small proportion of grains larger than 600 nm for MDF

* An attempt was already made to use conventional EBSD to study the present UFG cp-Ti and the spatial resolution was not high enough to map grains.

cp-Ti can be seen in Fig. 2b where the size-distribution histogram and the lognormal fit curve are presented. Similarly, a small proportion of grains larger than 1700 nm for ECAP cp-Ti can be seen in Fig. 2d. The presence of massively large-sized grains for both ECAP and MDF cp-Ti indicates that there was a microstructural inhomogeneity in as-deformed condition. The more effective grain refinement achieved by MDF, as shown by a much narrower peak together with smaller mean grain size in Fig. 2b, is probably due to the much higher deformation rate used in the former. A higher strain-rate tends to promote a more effective grain refinement [25]. The linear intercept method derived mean grain sizes was 623±71 nm for as-ECAP condition and 244±22 nm for as-MDF condition; these values agreed well with those as presented in Fig. 2d and 2b.

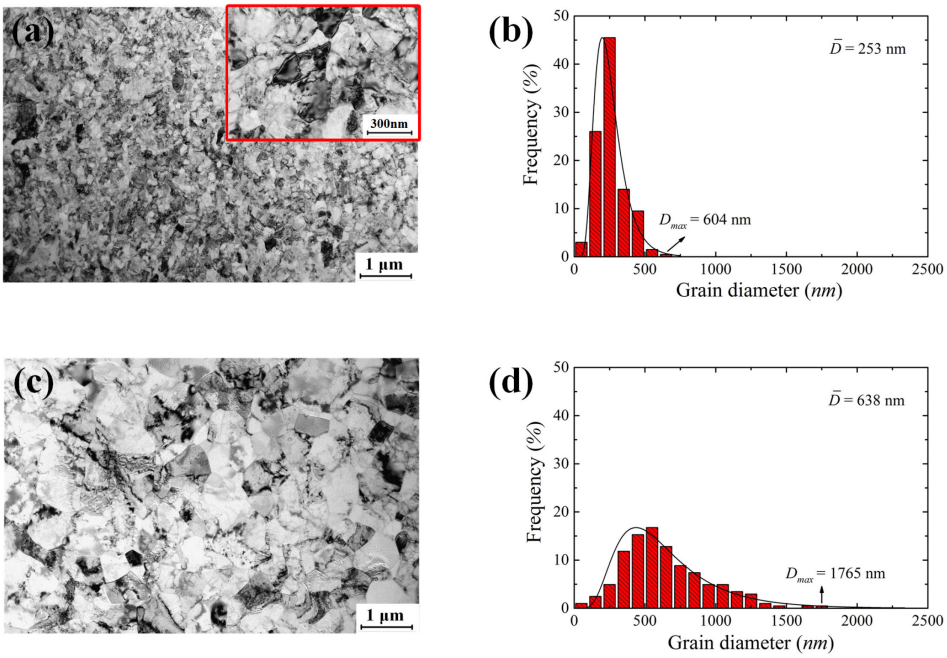

Fig. 2. Bright-field TEM micrographs and grain size-distribution histogram for two types of UFG cp-Ti processed by MDF method shown in (a) and (b), and ECAP shown in (c) and (d).

As expected, such a grain refinement led to improved static tensile strength but with some sacrifice in ductility, Table 1. Both the yield strength and tensile strength increased from 325 MPa and 416 MPa for as-received cp-Ti to 613 MPa and 705 MPa for MDF and to 597 MPa and 654 MPa for ECAP cp-Ti. The elastic limit was also determined from the static tensile stress-strain curve and the values are given in Table 1. It is clear that the stress amplitude of 280 MPa (Table 2) selected for all three *in situ* fatigue tests was well below the macro-scopic yield point.

The UFG microstructure created by both MDF and ECAP methods also exhibited a certain degree of deformation texture, as evidenced by the neutron diffraction spectra obtained from longitudinal and transversal directions. Representative neutron diffraction spectra obtained from specimen MDF-1 in pre-fatigue condition is shown in Fig. 1b. By comparison with transversal direction, the longitudinal direction revealed a strong diffraction peak from $\{10\bar{1}0\}$, but no {0002}, $\{10\bar{1}2\}$ $\{10\bar{1}3\}$ and $\{11\bar{2}2\}$, Fig. 1b. This indicates that for the MDF cp-Ti, a significant number of grains have their c-axis approx. perpendicular to the fatigue loading direction. In addition, ECAP cp-Ti showed a similar deformation texture (not shown for brevity) to the MDF cp-Ti; $\{10\bar{1}0\}$ grain family had the highest peak intensity accompanied by the absence of {0002} peak for the longitudinal direction.

3.2 *In situ* observation of HCF fatigue induced grain growth by neutron diffraction

Fig. 3a summarises the results of Pawley fitting in terms of the profile coefficient σ_{gauss} as a function of fatigue cycles. It is evident that except for MDF-1 that was fatigued at 25 °C, there was limited change in the magnitude of σ_{gauss} for MDF-2 (-200 °C) and ECAP (25 °C). This suggests that there was a significant grain size increase in MDF-1 (25 °C) and the grain growth particularly kicked in after 10^2 fatigue cycles. For the ECAP sample (25 °C), there was a measurable grain growth but the degree was much less compared to MDF-1 (25 °C). The higher value of σ_{gauss} for MDF cp-Ti compared with the ECAP one, Fig. 3a, is expected as the former had a much smaller mean grain size in the as-deformed condition (see $\overline{D}$ in Fig. 2b and 2d). Since the MDF cp-Ti shows the most noticeable grain growth due to the smaller grain size (Fig. 3a), the results presented in this paper are primarily confined to specimen MDF-1 that had been fatigued at 25 °C.

The relative intensity changes in MDF-1 (25 °C) are shown as a function of fatigue cycles in Fig. 3b for the longitudinal and in Fig. 3c for the transversal direction. In terms of longitudinal measurement, Fig. 3b, the intensity of all the diffraction peaks dropped with a similar proportion, suggesting an orientation-independent grain growth that occurred during HCF fatigue at 25 °C. In comparison, the transversal direction, Fig. 3c, reveal a progressive increase in {0002} grain family with fatigue cycles, whereas a limited decrease for $\{11\bar{2}0\}$ grain family. All the other

grain families showed a similar decrease, indicating the grain growth. As shown in Fig. 1b, the peak intensity for $\{11\bar{2}0\}$ grain family is the lowest among the all, thereby the statistical significance is low as the limited number of grains contributing to Bragg diffraction. The relative peak intensity increase for the {0002} grain family, as revealed by the transversal measurement data (Fig. 3b), suggests that the grain growth in UFG cp-Ti might exhibit an anisotropic behaviour. In fact, this interesting phenomenon can be shown more illustratively by comparing the diffraction spectra obtained at before and post-fatigued condition, Fig. 1c and 1d, where there was very limited change for the normalised peak intensity measured along the longitudinal direction, Fig. 1c, while almost all the other peaks disappeared except for the {0002} peak, Fig. 1d for the transversal direction. The microtexture analysis based on TKD measurements to be presented in section 3.4 were performed and a good agreement with the bulk neutron diffraction data was found. We also confirmed that no such a peak intensity drop was found for MDF-2 (-200 °C), indicating that the UFG microstructure is very stable when subjecting to a cryogenic-temperature HCF loading.

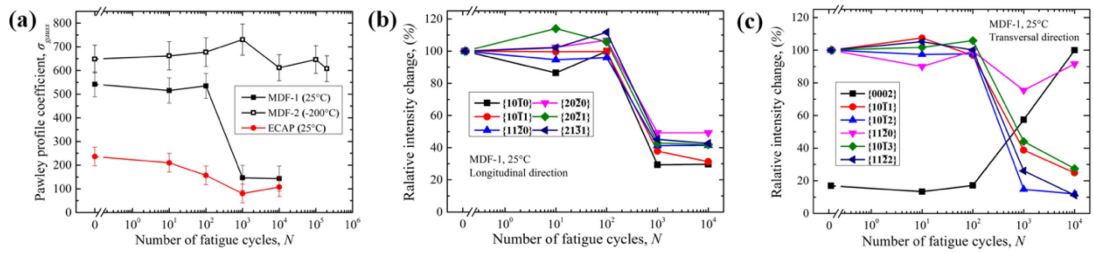

Fig. 3. (a) Pawley fitting obtained σ_{gauss} as a function of fatigue cycles for all three *in situ* tests showing the presence of noticeable grain size increase in MDF-1 that was fatigued at 25 °C; (b) and (c) single-peak fitting obtained relative peak intensity changes in MDF-1 for longitudinal and transversal directions, respectively. Note: The different peak intensities were normalised with respect to the initial value at 0 fatigue cycles, except for {0002} grain family where the peak was normalised with respect to the final value at 10^4 cycles.

An attempt was also made to compare the Gaussian peak width obtained by single-peak fitting applied to all three specimens MDF-1 (25 °C), MDF-2 (-200 °C) and ECAP (25 °C). The Gaussian peak width derived from the six major grain families did not exhibit any clear trend in terms of peak width broadening or shrinking as a function of fatigue cycles. This could be owing to the fact that titanium has a large negative neutron scattering length [26], causing a relatively low ratio of coherent scattering against incoherent scattering cross-section.

The Pawley fitting (Rietveld refinement analysis), applied to the complete diffraction spectrum, can also provide a measure of changes in the average lattice parameters [27], that is essentially a measure of macro-scopic internal strain if any yielding occurred during HCF fatigue loading. The macro-scopic internal strain was derived by comparing the measured lattice parameters, a, at each interrupted fatigue cycles, with the initially measured lattice parameter, a_0, at the reference condition. Similarly, intergranular lattice strains can be also determined via single-peak fitting. In this case, instead of using lattice parameter, the measured lattice spacing from each corresponding grain families was used to derive the intergranular strains. These are already standard data analysis procedures; more details can be found in [19].

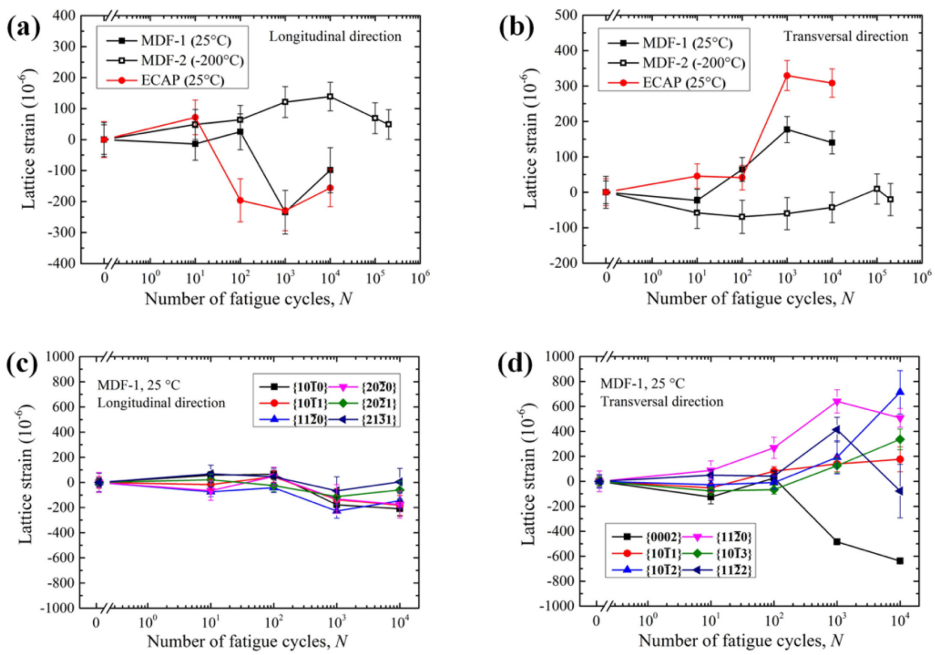

Fig. 4. (a) and (b) Pawley fitting obtained lattice strains as a function of fatigue cycles for all three *in situ* tests showing the absence of macro-scopic yielding for MDF-2 (-200 °C); (c) and (d) Single-peak fitting obtained intergranular strains in for MDF-1. (a) and (c) are measurements along the longitudinal direction, while (b) and (d) along the transversal direction.

Fig. 4a summarises the results of longitudinal residual lattice strains derived from lattice parameters for the three *in situ* HCF fatigue tests. Both MDF-1 (25 °C) and ECAP (25 °C) accumulated a macro-scopic internal strain of approx. -200 με at 10^4 fatigue cycles, whereas MDF-2 (-200 °C) had a value of +50 με at 2×10^5 cycles, Fig. 4a. Similarly, a measurable macro-scopic internal strain of +200 to +300 με was found for the transversal direction, Fig. 4b. It is important to note that the residual lattice strains built up during the present HCF fatigue are relatively small; when

expressed as stress it turns out to be ~20 MPa[†] in magnitude. This is in our expectation as the applied stress amplitude was well below the yield strength.

By examining each individual diffraction peaks for MDF-1 along longitudinal direction, the residual lattice strains for $\{10\bar{1}0\}$, $\{10\bar{1}1\}$ and $\{11\bar{2}0\}$ grain families were measured to be less than -200 με at 10^4 cycles, Fig. 4c. However, a very strong orientation-dependent lattice strain change can be seen in Fig. 4d for the transversal direction. It seems that the grain growth in MDF-1 during HCF fatigue caused a lattice strain relaxation (i.e. a stored energy release). This is generally agreed with the classic deformation and recrystallisation theory [28] where the newly recrystallised grains would release the stored strain energy. This indeed corroborates the peak intensity change for the {0002} grain family as revealed in Fig. 3c for the transversal detector bank.

In summary, *in situ* neutron diffraction data imply that fatigue deformation-induced grain growth occurred for specimen MDF-1 as a result of room-temperature R=-1 HCF fatigue, but such a grain growth was not found for MDF-2 in response to cryogenic-temperature HCF fatigue. The present experimental finding is a bit surprising as Zhang et al. [12] concluded that the grain growth in NC copper under indentation load at cryogenic-temperature was more significant than that under room-temperature indentation load. Their conclusion seems to be supported by molecular dynamics simulation in [29], where a rapid grain growth in NC copper was also claimed after subjecting the sample to a severe cyclic deformation at cryogenic temperature. To this end, additional experimental techniques, particularly those post-mortem characterisation tools, are required to first confirm the above-mentioned grain growth phenomenon revealed by *in situ* neutron diffraction and second provide complementary microstructural information to unravel the nature of grain growth.

3.3 Quantitative evaluation of grain growth during HCF fatigue

Fig. 5a, 5b and 5c present bright-field TEM micrographs of the cross-sectional plane[‡] of post-fatigued specimens MDF-1 (25 °C), MDF-2 (-200 °C) and ECAP (25 °C) respectively. It is evident that the post-fatigued MDF-1 had a much larger grain

[†] The typical value of diffraction elastic constants for hcp α-phase Ti is 115 to 140 GPa [39].
[‡] The TEM samples were extracted from the location where the neutron diffraction data were collected (i.e. within 1 mm distance the gauge volume centre position).

size, Fig. 5a, but the grain size in post-fatigued MDF-2 remained unchanged, Fig. 5b. The quantitative grain size evaluations are summarised in Fig. 5d, 5e and 5f for MDF-1, MDF-2 and ECAP, respectively. MDF cp-Ti had a grain size increase from 253 nm to 652 nm as a result of HCF fatigue loading at 25 °C, Fig. 5d. Hence, the TEM post-mortem grain size measurement result for MDF-1 (25 °C) confirmed what has been revealed through the *in situ* neutron diffraction, Fig. 3a. Furthermore, a very limited grain size increase from 253 nm to 305 nm was found for MDF-2 (-200 °C). Combining the neutron diffraction observation as shown in Fig. 3a and the TEM examination as shown in Fig. 5e, the present work provides unambiguous evidence to support that thermally activated process should play a vital role in triggering grain growth as HCF fatigue loading alone did not cause any significant grain growth. Finally, there was a limited increase in grain size from 638 nm to 699 nm for ECAP cp-Ti (25 °C), Fig. 5f.

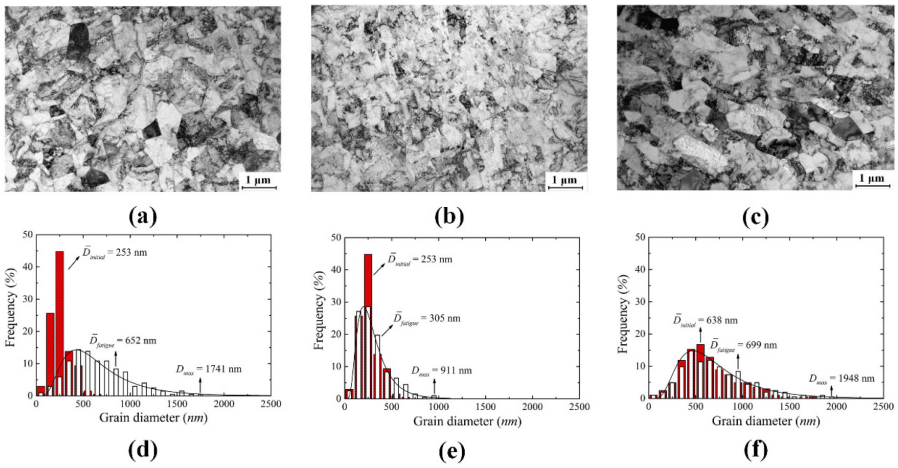

Fig. 5: The TEM micrographs in (a), (b) and (c) and grain-size distributions in (d), (e) and (f) for post-fatigued MDF and ECAP cp-Ti: (a) and (d) for MDF-1, 25 °C HCF fatigued at 4.3×10^4 cycles; (b) and (e) for MDF-2, -200 °C HCF fatigued at 2×10^5 cycles; (c) and (f) for ECAP, HCF fatigued at 4.8×10^4 cycles. The grain size distributions in pre-fatigued MDF and ECAP samples are also included in (d), (e) and (f) for a direct comparison.

Additional two off-line room-temperature fatigue tests were performed on MDF-deformed cp-Ti; they were stopped after 10^2 and 10^3 fatigue cycles. These two specimens were then cross-sectioned and representative TEM observations are shown in Fig. 6a and 6c. Fig. 6b and 6d show the grain size-distribution histograms as well as lognormal fit curves. The MDF-deformed sample had a mean grain size of 297 nm after 10^2 fatigue cycles, that is about 50 nm increase in size compared to the initial as-deformed condition, Fig. 6b, and the grain size further increased to 501 nm after 10^3

cycles, Fig. 6d. Fig. 7 presents grain size data (based on TEM micrographs) as well as micro-hardness data as a function of fatigue cycles for MDF-1 (25 °C). It can be seen in Fig. 7 that the grain growth during HCF fatigue loading of cp-Ti with the UFG microstructure was a continuous process. It is also noted that the gradual grain size increase with the increasing fatigue cycles agreed well with the reduction in micro-hardness value; indicating the loss of static strength due to grain coarsening.

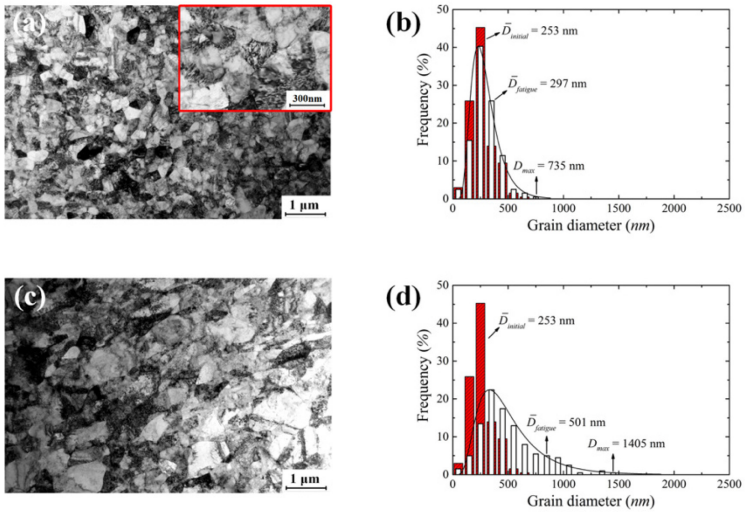

Fig. 6 Grain size-distribution histograms for MDF-deformed samples that were fatigued at 25 °C after 100 cycles in (a) and (b) and after 1000 cycles in (c) and (d).

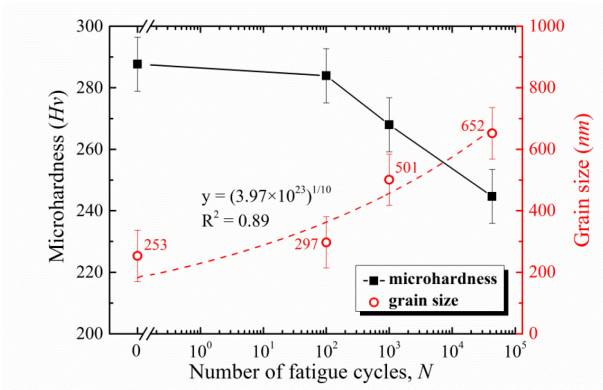

Fig. 7 Grain growth kinetics in MDF-deformed cp-Ti as a function of fatigue cycles at 25 °C. Also shown are the corresponding micro-hardness reduction and the Arrhenius-type grain growth law to emphasising the temperature-dependent nature of the presently observed grain growth.

3.4 Grain boundary character and texture changes during HCF fatigue

Fig. 8a and 8b show TKD crystal orientation maps for pre- and post-fatigued specimen MDF-1 respectively, while the corresponding pole figures are shown in Fig. 9a and 9b. The cross-sectional plane was examined, hence the results are corresponding to the longitudinal bank (Q∥). The considerable grain growth in MDF-

1 during HCF fatigue at 25 °C can be seen clearly in Fig. 8a and 8b. The mean grain size for pre-fatigued and post-fatigued MDF cp-Ti was determined to be 280 nm and 719 nm, confirming the grain growth that occurred during room-temperature HCF fatigue. These grain sizes derived based on TKD maps agreed reasonably well with those as determined based on TEM micrographs, see Fig. 5d. In addition, the {0001} pole figures as shown in Fig. 9a and 9b indicate that MDF cp-Ti developed a strong texture as a result of room-temperature HCF fatigue with the basal plane-normal (i.e. c-axis) perpendicular to the fatigue loading axis (i.e. Z-direction as indicated in the pole figure). The maximum texture intensity increased from 7.05 for the pre-fatigued to 12.48 for post-fatigued condition. This is consistent with the absence of neutron diffraction peak corresponding to {0002} grain families for both pre- and post-fatigued conditions, Fig. 1c.

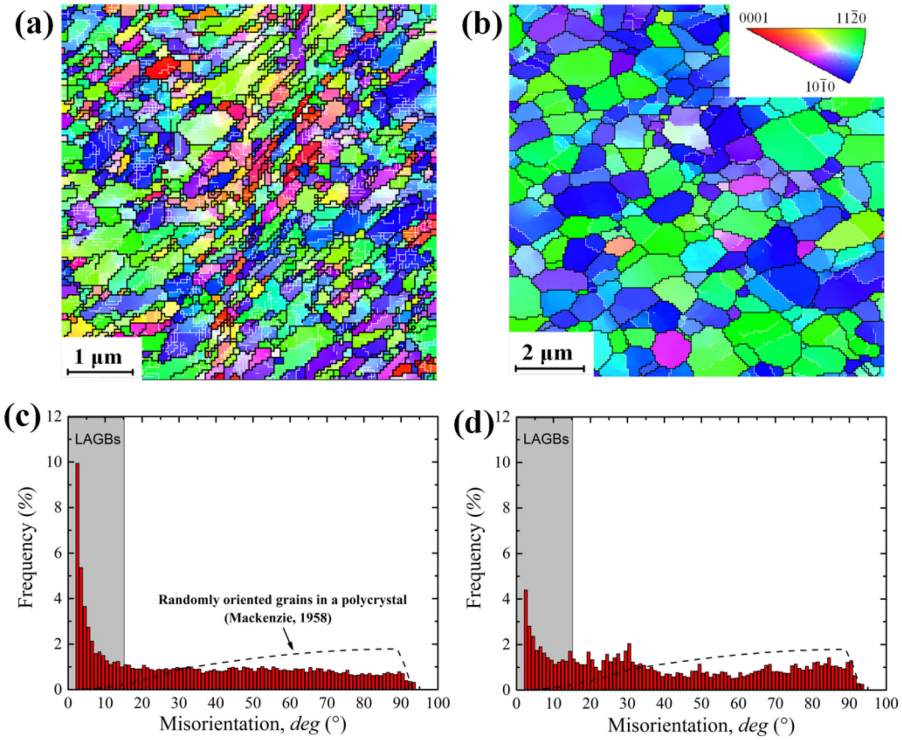

Fig. 8: TKD crystal-orientation maps in (a) and (b) and the derived fractions of HAGBs and LAGBs in (c) and (d) for MDF sample 1 tested under the HCF fatigue at 25 °C. (a) and (c) pre-fatigued condition; (b) and (d) post-fatigued condition. Note: the cross-sectional plane was examined, that is corresponding to the longitudinal direction of neutron diffraction ($Q_{\parallel}$).

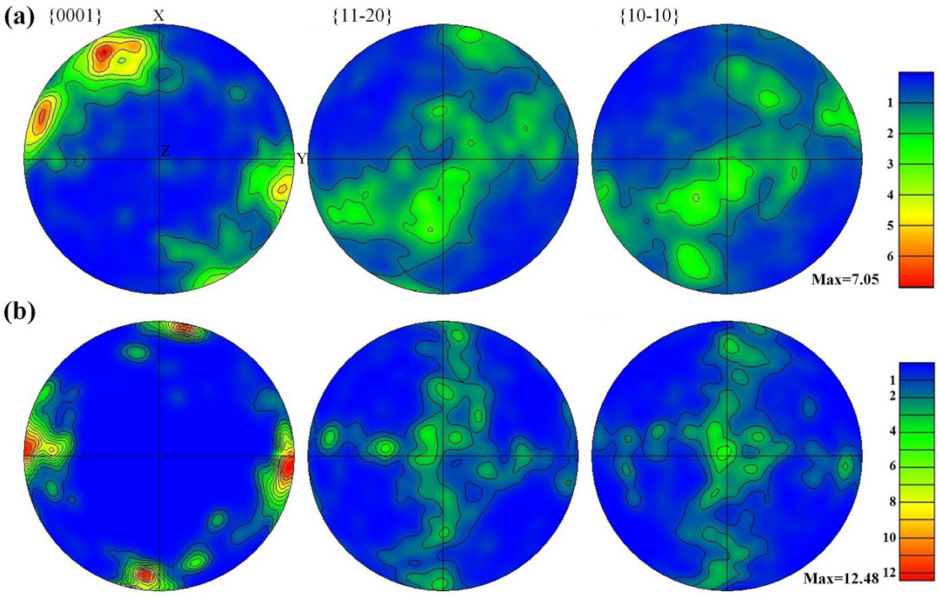

Fig. 9: The TKD pole figures obtained from examining the cross-sectional plane of the sample MDF-1 tested under the HCF fatigue at 25 °C. (a) is pre-fatigued condition, while (b) is post-fatigued condition. Note: the cross-sectional plane is corresponding to the longitudinal direction of neutron diffraction ($Q_{\parallel}$).

The interesting texture characteristic as revealed in Fig. 9b when examining the cross-sectional plane of HCF fatigued MDF-1 also led us to postulate that there should be a strong texture of {0001} at the pole figure centre location if the longitudinal plane is examined. To this end, additional TKD sample was prepared to examine the texture from the longitudinal plane and the results are shown in Fig. 10 and Fig. 11. This indeed provided the grain growth and texture information corresponding to the transversal bank ($Q_{\perp}$). As expected, there is a very strong {0001} texture at the centre position of pole figure with the maximum intensity of 22.56 in Fig. 11b for the post-fatigued condition. Again, this confirms the relative peak intensity increase for {0002} grain family as revealed in Fig. 1d and Fig. 3c. The TKD orientation map of post-fatigued MDF-1 in Fig. 10b shows evidently that a significant proportion of the coarsened grains has a preferred orientation with their c-axis perpendicular to the fatigue loading direction. More detailed discussions about this orientation-dependent grain growth phenomenon will be given in section 4.3.

Based on Fig. 8a and 8b as well as Fig. 10a and 10b, the mean grain size for pre-fatigued MDF-1 was determined to be 280 nm for cross-sectional plane and 445 nm for longitudinal plane, respectively, while the grain sizes reached to 719 nm and 906 nm for post-fatigued condition, confirming the grain growth that occurred during room-temperature HCF fatigue.

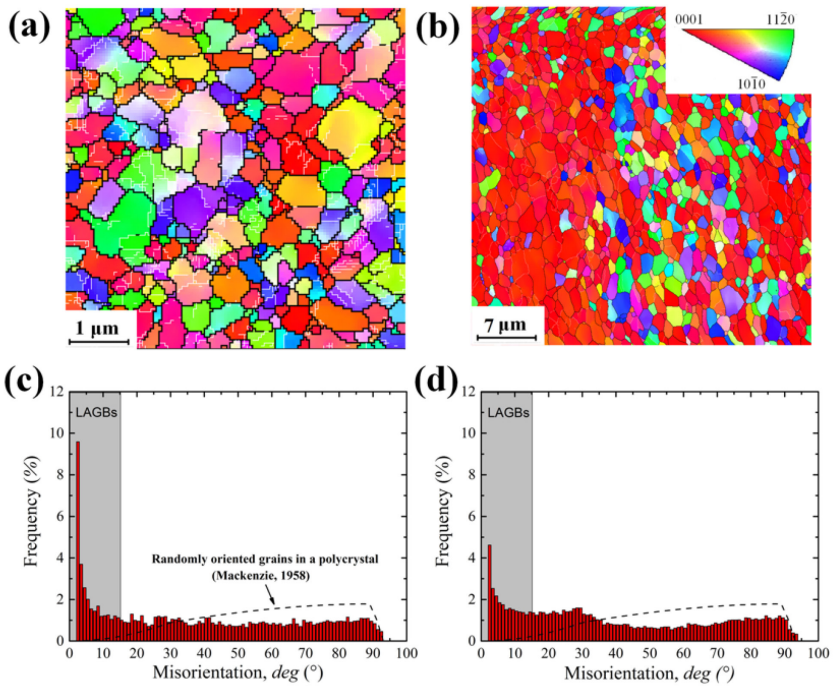

Fig. 10: TKD crystal-orientation maps in (a) and (b) and the derived fractions of HAGBs and LAGBs in (c) and (d) for MDF sample 1 tested under the HCF fatigue at 25 °C. (a) and (c) pre-fatigued condition; (b) and (d) post-fatigued condition. Note: the longitudinal plane was examined, that is corresponding to the transversal direction of neutron diffraction ($Q_{\perp}$).

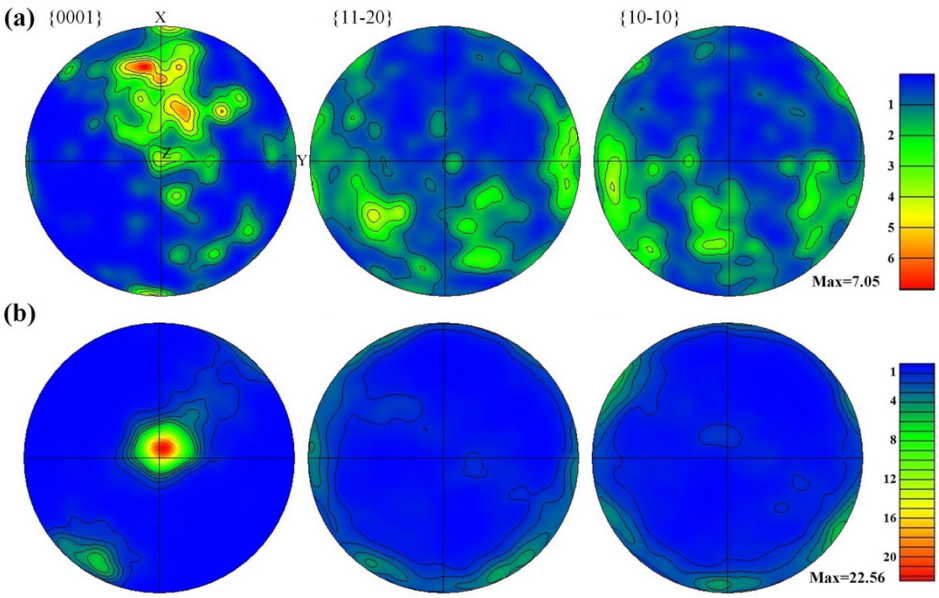

Fig. 11: The TKD pole figures obtained by examining the longitudinal plane of the sample MDF-1 tested under the HCF fatigue at 25 °C. (a) is pre-fatigued condition, whereas (b) is post-fatigued condition.

The fraction of different types of grain boundaries were evaluated based on the TKD maps. In the TKD maps of Fig. 8a, 8b, 10a and 10b, LAGBs were depicted as white lines, while HAGBs as black lines. Grain boundaries with misorientation

angles between 2° and 15° were defined as LAGBs and those of misorientation angles >15° as HAGBs. The misorientation angle distribution of MDF-1 in pre-fatigued and post-fatigued conditions are shown in Fig. 8c and 8d, for the cross-sectional plane. Compared with the pre-fatigued condition (Fig. 8c), there is a significant decrease in the frequency of the LAGBs accompanied by the increase in the frequency of HAGBs, Fig. 8d. A similar reduction in the frequency of the LAGBs due to room-temperature fatigue can be seen for the longitudinal plane, Fig. 10c and 10d.

4. Discussion

We now discuss our experimental observations with respect to (i) the grain growth mechanism associated with HCF fatigue deformation; (ii) the interrelationship between deformation modes and grain growth; and (iii) anisotropic grain growth behaviour.

4.1 The mechanism of grain growth during HCF fatigue deformation

The transition from LAGBs to HAGBs as revealed from both observation planes (Fig. 8c, 10c for pre-fatigued and Fig. 8d and 10d for post-fatigued conditions) suggests that continuous dynamic recrystallisation acts as the grain growth mechanism during room-temperature HCF fatigue of UFG cp-Ti. This is consistent with the previous work where an ECAP interstitial-free steel was studied during subsequent isothermal annealing [30] where the continuous recrystallisation was claimed to be responsible for the homogeneous grain coarsening. Moreover, the high fraction of severe plastic deformation induced HAGBs (65.6% and 70.4%, Fig. 8c and Fig. 10c) for MDF cp-Ti in pre-fatigued condition also shows a very good agreement with the critical proportion of HAGBs (62 to 64% as reported by Jazaeri and Humphreys [23,31]) that triggers the transition from discontinuous to continuous recrystallisation. The primary difference between continuous and discontinuous recrystallisation is that the grain microstructure evolves relatively homogeneous through the whole material for the former. Hence it is impossible to separate the already recrystallised and non-recrystallised regions. As shown in Fig. 8b and 10b, the post-fatigued microstructure is homogeneous and without any discernible non-recrystallised regions.

Grain growth kinetics can also be derived from the grain size data as presented in Fig. 7. In the isothermal annealing work by Hazra et al. [30] on ECAP steel, the grain coarsening kinetics was derived following the relation:

$$\overline{D}^n = kt \quad (1)$$

where $\overline{D}$ is the mean grain size, k is a temperature-dependent rate constant and n is the grain/sub-grain growth exponent. In the present case for cyclically loaded MDF-1, we accordingly replace the time t in Eq. 1 with fatigue cycles N (i.e. cycle-dependent). As presented in Fig. 7, a value of n=10 was obtained. This suggests that the grain coarsening process was controlled by a recovery-involved recrystallisation mechanism as revealed in ECAP steel under isothermal annealing [30] where large n values of between 5 and 13 were found for the grain growth kinetics.

Because the fatigue-induced grain growth was very commonly reported to occur locally near the crack surfaces (e.g. the work on ECAP copper [32], electro-deposited NC nickel, [3] and NC platinum films [9]), the large strains in a cyclic plastic zone around the crack tip should be responsible for this phenomenon. This explanation seems to be supported by the fatigue work by Hoppel et al. [7] where cyclic deformation-induced grain coarsening in ECAP copper was found to be enhanced with the increasing plastic strain amplitude in HCF fatigue regime. However, for the tests performed at intermediate plastic strain ranges (involving more fatigue cycles, i.e. a longer time), the degree of grain coarsening increased with decreasing plastic strain amplitude. The time-dependency of such a process probably implies a thermally activated process.

In this regard, the present *in situ* neutron diffraction observations provide an unambiguous evidence that the grain growth in fatigued UFG cp-Ti was a thermally activated continuous recrystallisation process which already occurred at room temperature, Fig. 3a. At first glance, this key experimental finding does not support the atomic-scale computer simulation work [29] where grain growth was found to be solely driven by cyclic stress/strain, instead of temperature/thermal energy. The so-called *stress-driven grain growth* was firstly proposed based on the work by Weertman's group [12,33] where a rapid grain growth in NC copper thin films under cryogenic-temperature indentation load was found in contrast to room-temperature

indentation. As already mentioned by Jin et al. [34], one should acknowledge the limitations of *in situ* experiments on thin film type NC samples as the stress can be relieved by deformation perpendicular to the foil, a mechanism that would not be available in bulk samples. In addition, the NC metals with less than 100 nm grain size have very limited discrete dislocations within grains and are very unlikely to form dislocation cells/sub-grains. This could explain why the grain growth is often assisted by grain boundary dislocations that involve the stress-induced grain rotation and then grain coalescence [34,35]. Therefore, the present experimental evidence in supporting the role of thermal activation on grain growth in UFG cp-Ti in response to room-temperature HCF fatigue (possibly also applies for other UFG metals) should not be judged as in conflict with the *stress-driven grain growth* process in NC metals.

The present *in situ* neutron diffraction results have been confirmed by both TEM and TKD based post-mortem characterisations. Hence, the thermal activation of grain growth in response to room-temperature HCF fatigue loading needs to be considered when studying small-grained metals, although a growing number of investigations revealed *stress-driven grain growth* process as an efficient mechanism to accommodate plastic deformation. Investigations into the *intrinsic* fatigue behaviour of metals with the UFG microstructure are challenging as they tend to have limited thermal stability. Hence the comparison with the cryogenic-temperature HCF fatigue certainly helps to clarify the underlying mechanism in grain growth by limiting the role of diffusion rate. By performing the identical HCF fatigue test at cryogenic temperature (MDF-2), it is evident that the grain growth is very sluggish, Fig. 3a and Fig. 5e.

Furthermore, such an HCF fatigue induced grain growth in UFG cp-Ti already begun within the first 100 fatigue cycles for MDF-1 (Fig. 3a and Fig. 7), hence it is less likely that a solid amount of incubation time is required, but the rate of grain coarsening is strongly dependent on the initial stored energy by severe plastic deformation (i.e. the degree of grain refinement, comparing ECAP and MDF-1 in Fig. 5d and Fig. 5f). Formation of non-equilibrium grain boundaries containing numerous dislocations within grain boundaries (i.e. sub-grains) in UFG metals is an immediate consequence of severe plastic straining. The non-equilibrium grain boundaries are manifested by the existence of high energy, excess defect volume, and long-range stress field [1]. Accordingly, the rate of atomic transport in UFG metals is enhanced by many orders of magnitude compared to that in coarse-grained metals because of

the large number of diffusion paths. This could explain why the grain growth already occurred at a relatively low homologous temperature (i.e. room temperature). It is also important to note that the thermal conductivity of pure titanium is 17 W/mK, which is much lower than that of iron, copper and nickel. This indicates that under HCF fatigue loading, the UFG cp-Ti is easy to warm.

The dynamically recrystallised grains are expected to have a lower dislocation density compared with the severe plastic deformation induced UFG microstructure. This means that one should expect to see a much lower value of geometrically necessary dislocations (GND) in post-fatigued MDF-1. Local crystal orientations on MDF-1 sample, before and after HCF fatigue, were measured to study the GND density change. Any local misorientation angle calculated greater than 2° was excluded. The kernel average misorientation (KAM) method was used to determine the local misorientation based on the TKD orientation maps as shown in Fig. 8a, 8b for cross-sectional plane and Fig. 10a and 10b for longitudinal plane. A detailed description for the determination of GND density can be found elsewhere [36]. For the present cp-Ti, the magnitude of Burgers vector *b* of 0.289 nm was used. In terms of the cross-sectional plane, the average GND value decreased from 2.43×10^{15} m^{-2} to 1.16×10^{15} m^{-2} as a result of HCF fatigue for MDF-1. A similar decrease from 2.00×10^{15} m^{-2} to 8.87×10^{14} m^{-2} was found for the longitudinal plane. Hence, the GND density reduction is another evidence to support that continuous dynamic recrystallisation is responsible for the room-temperature HCF fatigue induced grain growth in cp-Ti with UFG microstructure.

4.2 Deformation modes and grain growth

It is generally agreed that the primary basal $\{0002\}\langle 11\bar{2}0\rangle$ or prismatic $\{10\bar{1}0\}\langle 11\bar{2}0\rangle$ slip systems are not capable of accommodating plastic deformation along the c-axis for the hcp α-phase in titanium and its alloys [37]. Hence either twinning [38] or <c+a> slip modes operating on the $\{10\bar{1}1\}$ and $\{11\bar{2}2\}$ planes are required to ensure full plasticity [39]. By using *in situ* synchrotron X-ray diffraction combined with tensile deformation on Ti-6Al-4V, it was reported by Stapleton et al. [37] that $\{10\bar{1}2\}$ grain family is the first to exhibit micro-yielding, followed by $\{10\bar{1}1\}$, $\{20\bar{2}1\}$ and $\{10\bar{1}3\}$ grain families. Since very small magnitudes of lattice

strains were accumulated for $\{10\bar{1}1\}$ and $\{20\bar{2}1\}$ grain families at the end of fatigue cycles, Fig. 4c, it is very unlikely that micro-yielding at these soft oriented grains already occurred in the fatigued MDF-1 cp-Ti. Note both the diffraction peaks corresponding to $\{10\bar{1}2\}$ and $\{10\bar{1}3\}$ grain families were not found for the longitudinal bank measurement, due to the deformation texture associated with the severe plastic deformation means.

The second reason that helps to rule out the dislocation slip involved grain growth is laid out below. As a consequence of room-temperature HCF fatigue, the grain size increased from 253 nm to 652 nm for MDF-1 (Fig. 5d), this might suggest that some micro-yielding could have already occurred due to the continuous material softening as revealed by the hardness drop in Fig. 7. However, for the ECAP cp-Ti that has the initial grain size of 638 nm (Fig. 5f), the elastic limit is 544 MPa (Table 1). This means that even for the post-fatigued MDF-1 having a grain size of 652 nm (similar to the initial grain size of ECAP), the elastic limit should be much higher than the applied fatigue stress amplitude of 280 MPa. It is thus concluded that the grain growth observed here is very unlikely to be related to the dislocation slip process.

Furthermore, nanotwins-assisted grain growth phenomenon was found in 20-nm-thick gold films with an initial grain size of ~19 nm under room-temperature HCF and LCF fatigue loading (R=0.1) [40]. Since deformation twinning is strongly sensitive to grain size [41], the influence of grain size on deformation twining and vice versa are of particular attention for the present UFG cp-Ti as their grain sizes evolves under a R=-1 fatigue loading cycles. To this end, it is worthwhile to re-visit neutron diffraction spectra along both the longitudinal and transversal directions with the primary focus to examine the relative peak intensity changes associated with the parent and twinned grains.

The two detector banks set up at ENGIN-X instrument as illustrated in Fig. 1a is well known to be suitable for studying deformation tensile twinning (e.g. cp-Ti in [38] and Mg in [41]). At first glance of Fig. 3d that illustrates the peak intensity changes for transversal direction before and after the HCF fatigue, one might think the increase in peak intensity from {0002} grain family is in accordance to the decrease in peak intensity from $\{10\bar{1}1\}$ grain family. However, they are not a pair of parent and twinned grains. Actually, the activation of tensile twinning creates an almost 90° reorientation of the parent grains that include $\{10\bar{1}0\}$ and $\{11\bar{2}0\}$ grains with their

plane-normal parallel to the loading axis. If there is any deformation twinning activated, the longitudinal bank is expected to show clear increases in the peak intensity for {0002} and $\{10\bar{1}3\}$ grain families, accompanied by the peak intensity decrease from parent grains of $\{10\bar{1}0\}$ and $\{11\bar{2}0\}$ orientations. This is obviously not the case as shown in Fig. 3a where all diffraction peaks showed similar magnitude of the peak intensity decrease. The diffraction spectrum, obtained from the longitudinal bank, Fig. 1c, for the post-fatigued MDF-1 showed evidently that there was no measurable peaks for {0002} and $\{10\bar{1}3\}$ grain families. Similarly, the transversal bank did not show the expected peak intensity increase for $\{10\bar{1}0\}$ and $\{11\bar{2}0\}$ grain families accompanied with the decrease for {0002} and $\{10\bar{1}3\}$ peaks, if there was any deformation-twinning occurred during the HCF fatigue. To this end, we have re-affirmed that the deformation twinning cannot explain the abnormal peak intensity increase for the {0002} grain family in Fig. 3d.

4.3 Anisotropic grain growth

In the work on ECAP magnesium [42], the {0001} pole figure showed the formation of a maximum located at 45° from extrusion direction, indicating that the basal planes rotated during ECAP to a position parallel to the shear direction. Hence the present deformation texture in severe plastically deformed MDF cp-Ti, Fig. 1b and Fig. 11a is consistent with the previous work. The subtle difference here is that the MDF cp-Ti showed a certain portion of grains with their c-axis perpendicular to the longitudinal axis of MDF process, see the indicated Z-direction in Fig. 11a.

Since the fatigue sample was extracted in such a way that the loading axis was parallel to the MDF sample longitudinal axis, this means that the basal planes of the majority of the grains were well positioned to allow the <a> slip mode activation with respective to the loading direction. In other words, the initial MDF deformation texture should not be judged to limit the activation of <a> slip system, which is different to the case that the load was applied parallel to the rolling direction for a heavily rolled hcp-metal [42]. As a result, the so-called rotational recrystallisation mechanism [42–44] could be thought to be responsible for the present dramatic change (~45° around the c-axis comparing Fig. 11a and 11b) in texture before and after the HCF fatigue-induced grain growth.

The rotational recrystallisation mechanism, proposed initially by Ion et al. [43] and modified by del Valle and Ruano [42] on hcp structured magnesium alloys, would require the following dislocation slip involved steps: under compression the slip in the basal planes produces a kinking of the lattice close to the grain boundary and the rotation of basal planes in the new recrystallised grains is hence more towards a position with the c-axis at higher tilt with respect to the compression axis (basal plane more parallel to the compression axis). In contrast, under tension the new recrystallised grains tend to have their c-axis at lower tilt with respect to the tensile axis (basal plane more perpendicular to the tensile axis). As already discussed in section 4.2, dislocation slip is very unlikely in the present case. Even though such a rotational recrystallisation process occurred, the applied fully reversed R=-1 fatigue load would cause an equal chance to rotate the grains towards and away from the load axis. No significant lattice rotation should be expected for the post-fatigued sample.

The orientation difference of the recrystallised microstructure, Fig. 11b, and as-deformed UFG microstructure, Fig. 11a, is likely to be a consequence of anisotropic grain growth behaviour where the {0001} grain family with their c-axis perpendicular to the fatigue load axis grew much faster at the expense of other grain families. The underlying reason for such an orientation dependency is probably related to the recrystallisation nucleation probability [28]. The nucleation probability increases with the stored plastic energy of the differently orientated grains. For the present cp-Ti, a typical hcp metal, due to the lower crystal symmetry and smaller number of available slip systems, the severe plastic deformation would readily cause a stronger orientation dependence of accumulated strain energy, i.e. more plastically anisotropy than cubic metals. In this sense, the grains having their c-axis towards the direction perpendicular to the longitudinal axis of MDF process means that those grains would have accumulated highly stored energy due to severe plastic deformation. Accordingly, the recrystallisation nucleation occurred in these highly deformed {0001} grain families, the stored energy in these grains were consequently released but the crystallographic orientation of the recrystallised grains would be preserved. Indeed, the presence of transversal lattice strain changes accompanying the grain growth behaviour, Fig. 4b, but absence of such changes for the longitudinal bank in Fig. 4a, provide some evidence to support that recrystallisation nucleation is favoured from those grains with high stored energy.

5. Conclusions

Here we report a clear experimental evidence that continuous grain growth in UFG cp-Ti occurred during room-temperature HCF fatigue loading and no noticeable grain growth was detected for the cryogenic-temperature HCF fatigue. Based on both *in situ* neutron diffraction measurements as well as post-mortem microstructural characterisations, the main conclusions can be drawn for UFG cp-Ti:

1) The thermally activated (diffusional) process should play a significant role in triggering grain growth during HCF fatigue loading.
2) For the MDF cp-Ti, the UFG microstructure is rather unstable and undergoes a continuous grain growth as a function of room-temperature HCF fatigue cycles.
3) Continuous dynamic recrystallisation is responsible for the grain coarsening in response to room-temperature HCF fatigue.
4) There was no evidence to suggest that the grain growth in cp-Ti with UFG microstructure in response to HCF fatigue loading is a result of dislocation slip or twinning process.
5) The anisotropic grain growth behaviour in {0002} grain family can be explained by accepting that this particular grain orientations tended to accumulate higher stored energy during severe plastic deformation and recrystallisation nucleation occurred in these highly deformed regions.

Acknowledgement

Bo Chen acknowledges UK EPSRC for financial support through grants EP/P025978/1 and EP/R043973/1. The authors acknowledge the ISIS beam time award RB1710270 and ISIS Newton Programme. This work was funded by NSFC of China (51725503, 51605164). The authors are also grateful to the Suqian Research Institute of Hohai University and Guangxi University in processing UFG cp-Ti and the Electron Microscope Centre of Chongqing University with the assistance of TKD analysis. We also extend our thank you to Ranggi Ramadhan and Yao Li for their participations in neutron diffraction experiment.

References

[1] R.Z. Valiev, R.K. Islamgaliev, I. V Alexandrov, Bulk nanostructured materials from severe plastic deformation, Prog. Mater. Sci. 45 (2000) 103–189.

[2] H. Mughrabi, H.W. Hoppel, M. Kautz, Fatigue and microstructure of ultrafine-grained metals produced by severe plastic deformation, Scr. Mater. 51 (2004) 807–812.

[3] B.L. Boyce, H.A. Padilla, Anomalous Fatigue Behavior and Fatigue-Induced Grain Growth in Nanocrystalline Nickel Alloys, Metall. Mater. Trans. A. 42 (2011) 1793–1804.

[4] M.W. Kapp, T. Kremmer, C. Motz, B. Yang, R. Pippan, Structural instabilities during cyclic loading of ultrafine-grained copper studied with micro bending experiments, Acta Mater. 125 (2017) 351–358.

[5] S. Kobayashi, A. Kamata, T. Watanabe, A mechanism of grain growth-assisted intergranular fatigue fracture in electrodeposited nanocrystalline nickel – phosphorus alloy, Acta Mater. 91 (2015) 70–82.

[6] A.B. Witney, P.G. Sanders, J.R. Weertman, J.A. Eastman, Fatigue of nanocrystalline copper, Scr. Metall. Mater. 33 (1995) 2025–2030.

[7] H.W. Hoppel, Z.M. Zhou, H. Mughrabi, R.Z. Valiev, Microstructural study of the parameters governing coarsening and cyclic softening in fatigued ultrafinegrained copper, Philos. Mag. A. 82 (2002) 1781–1794.

[8] S. Cheng, Y. Zhao, Y. Wang, Y. Li, X. Wang, P.K. Liaw, E.J. Lavernia, Structure Modulation Driven by Cyclic Deformation in Nanocrystalline NiFe, Appl. Phys. Lett. 104 (2010) 255501.

[9] R.A. Meirom, D.H. Alsem, A.L. Romasco, T. Clark, R.G. Polcawich, J.S. Pulskamp, M. Dubey, R.O. Ritchie, C.L. Muhlstein, Fatigue-induced grain coarsening in nanocrystalline platinum films, Acta Mater. 59 (2011) 1141–1149.

[10] R.Z. Valiev, Nanostructuring of metals by severe plastic deformation for advanced properties, Nat. Mater. 3 (2004) 511–516.

[11] A. Vinogradov, S. Hashimoto, Multiscale phenomena in fatigue of ultra-fine grain materials - an overview, Mater. Trans. 42 (2001) 74–84.

[12] K. Zhang, J.R. Weertman, J.A. Eastman, Rapid stress-driven grain coarsening in nanocrystalline Cu at ambient and cryogenic temperatures, Appl. Phys. Lett.

87 (2005) 061921.
[13] L. Wang, Y.C. Wang, A.P. Zhilyaev, A. V. Korznikov, S.K. Li, E. Korznikova, T.G. Langdon, Microstructure and texture evolution in ultrafine-grained pure Ti processed by equal-channel angular pressing with subsequent dynamic compression, Scr. Mater. 77 (2014) 33–36.
[14] V. V Stolyaro, Y.T. Zhu, I. V Alexandro, T.C. Lowe, R.Z. Valie, Grain refinement and properties of pure Ti processed by warm ECAP and cold rolling, Mater. Sci. Eng. A. 343 (2003) 43–50.
[15] V.M. Segal, Materials processing by simple shear, Mater. Sci. Eng. A. 197 (1995) 157–164.
[16] W.I.F. David, J.D. Jorgensen, Rietveld refinement with time-of-flight powder diffraction data from pulsed neutron sources, in: Proc. Int. Work. Rietveld Method, Petten, 1990.
[17] G.S. Pawley, Unit-cell refinement from powder diffraction scans, J. Appl. Cryst. 14 (1981) 357–361.
[18] A.L. Patterson, The Scherrer formula for X-ray particle size determination, Phys. Rev. 56 (1939) 978–982.
[19] B. Chen, J.N. Hu, P.E.J. Flewitt, D.J. Smith, A.C.F. Cocks, S.Y. Zhang, Quantifying internal stress and internal resistance associated with thermal ageing and creep in a polycrystalline material, Acta Mater. 67 (2014) 207–219.
[20] B. Chen, J.N. Hu, Y.Q. Wang, S.Y. Zhang, S. Van Petegem, A.C.F. Cocks, D.J. Smith, Role of the misfit stress between grains in the Bauschinger effect for a polycrystalline material, Acta Mater. 85 (2015) 229–242.
[21] M. Ferry, N. Burhan, Structural and kinetic aspects of continuous grain coarsening in a fine-grained Al – 0.3Sc alloy, 55 (2007) 3479–3491.
[22] H. Sharma, D. Parfitt, A.K. Syed, D. Wimpenny, E. Muzangaza, G. Baxter, B. Chen, A critical evaluation of the microstructural gradient along the build direction in electron beam melted Ti-6Al-4V alloy, Mater. Sci. Eng. A. 744 (2019) 182–194.
[23] H. Jazaeri, F.J. Humphreys, The transition from discontinuous to continuous recrystallization in some aluminium alloys I - The deformed state, Acta Mater. 52 (2004) 3239–3250.
[24] M. Meisnar, A. Vilalta-clemente, A. Gholinia, M. Moody, A.J. Wilkinson, N. Huin, S. Lozano-perez, Using transmission Kikuchi diffraction to study

intergranular stress corrosion cracking in type 316 stainless steels, Micron. 75 (2015) 1–10.

[25] K. Wang, N.R. Tao, G. Liu, J. Lu, K. Lu, Plastic strain-induced grain refinement at the nanometer scale in copper, 54 (2006) 5281–5291.

[26] A. Dianoux, G. Lander, Neutron Data Booklet, Institut Laue-Langevin, OCP Science imprint, 2003.

[27] M.R. Daymond, M.A.M. Bourke, R.B. Von Dreele, B. Clausen, T. Lorentzen, Use of Rietveld refinement for elastic macrostrain determination and for evaluation of plastic strain history from diffraction spectra, J. Appl. Phys. 82 (1997) 1554–1562.

[28] D.E. Solas, C.N. Tomé, O. Engler, H.R. Wenk, Deformation and recrystallization of hexagonal metals: Modeling and experimental results for zinc, Acta Mater. 49 (2001) 3791–3801.

[29] J. Schiotz, Strain-induced coarsening in nanocrystalline metals under cyclic deformation, Mater. Sci. Eng. A. 375–377 (2004) 975–979.

[30] S.S. Hazra, E. V. Pereloma, A.A. Gazder, Microstructure and mechanical properties after annealing of equal-channel angular pressed interstitial-free steel, Acta Mater. 59 (2011) 4015–4029.

[31] H. Jazaeri, F.J. Humphreys, The transition from discontinuous to continuous recrystallization in some aluminium alloys II - annealing behaviour, Acta Mater. 52 (2004) 3251–3262.

[32] A. Vinogradov, T. Kawaguchi, Y. Kaneko, S. Hashimoto, Fatigue crack growth and related microstructure evolution in ultra fine grain copper processed by ECAP, Mater. Trans. 53 (2012) 101–108.

[33] Z. Huang, L.Y. Gu, J.R. Weertman, Temperature dependence of hardness of nanocrystalline copper in low-temperature range, Scr. Mater. 37 (1997) 1071–1075.

[34] M. Jin, A.M. Minor, E.A. Stach, J.W. Morris, Direct observation of deformation-induced grain growth during the nanoindentation of ultrafine-grained Al at room temperature, Acta Mater. 52 (2004) 5381–5387. doi:10.1016/j.actamat.2004.07.044.

[35] Y.B. Wang, B.Q. Li, M.L. Sui, S.X. Mao, Deformation-induced grain rotation and growth in nanocrystalline Ni, Appl. Phys. Lett. 92 (2008) 011903.

[36] X. Ma, C. Huang, J. Moering, M. Ruppert, H.W. Höppel, M. Göken, J.

Narayan, Y. Zhu, Mechanical properties of copper/bronze laminates: Role of interfaces, Acta Mater. 116 (2016) 43–52.

[37] A.M. Stapleton, S.L. Raghunathan, I. Bantounas, H.J. Stone, T.C. Lindley, D. Dye, Evolution of lattice strain in Ti-6Al-4V during tensile loading at room temperature, Acta Mater. 56 (2008) 6186–6196.

[38] D. Gloaguen, G. Oum, V. Legrand, J. Fajoui, S. Branchu, Experimental and theoretical studies of intergranular strain in an alpha titanium alloy during plastic deformation, Acta Mater. 61 (2013) 5779–5790.

[39] J.L.W. Warwick, J. Coakley, S.L. Raghunathan, R.J. Talling, D. Dye, Effect of texture on load partitioning in Ti-6Al-4V, Acta Mater. 60 (2012) 4117–4127.

[40] X. Luo, X. Zhu, G. Zhang, Nanotwin-assited grain growth in nanocrystalline gold films under cyclic loading, Nat. Commun. 5 (2014) 1–8.

[41] O. Muransky, M.R. Barnett, D.G. Carr, S.C. Vogel, E.C. Oliver, Investigation of deformation twinning in a fine-grained and coarse-grained ZM20 Mg alloy : Combined in situ neutron diffraction and acoustic emission, Acta Mater. 58 (2010) 1503–1517.

[42] J.A. del Valle, O.A. Ruano, Influence of texture on dynamic recrystallization and deformation mechanisms in rolled or ECAPed AZ31 magnesium alloy, Mater. Sci. Eng. A. 487 (2008) 473–480.

[43] S.E. Ion, F.J. Humphreys, S.H. White, Dynamic recrystallisation and the development of microstructure during the high temperature deformation of magnesium, Acta Metall. 30 (1982) 1909–1919.

[44] S. Biswas, B. Beausir, L.S. Toth, S. Suwas, Evolution of texture and microstructure during hot torsion of a magnesium alloy, Acta Mater. 61 (2013) 5263–5277.